Jurnal Ilmiah Teknik Elektro Komputer dan Informatika (JITEKI)
Vol. 10, No. 4, December 2024, pp. 763–774
ISSN: 2338-3070, DOI: 10.26555/jiteki.v10i4.30191 

# Estimation of $R_o$ and $V_c$ Parameters Using Recursive Least Square, as Well as $OCV$ Parameters at Rest Conditions in Pulse Test for the Thevenin Battery Model Implemented on Raspberry Pi Zero

Paris Ali Topan, Dinda Fardila
Universitas Teknologi Sumbawa, Indonesia

**ARTICLE INFO**

**Article history:**

Received September 30, 2024
Revised November 29, 2024
Published December 20, 2024

**Keywords:**

Lithium Polymer Battery;
Thevenin Model;
Recursive Least Squares;
Pulse Test;
Raspberry pi

**ABSTRACT**

Lithium polymer (Li-Po) batteries are one of the most widely used batteries, especially on everyday devices such as mobile phones and laptops. One of the main reasons for using this type of Lithium battery is its high energy density. In its use, this battery needs to be monitored to prevent unwanted things from happening. A model is needed to describe the characteristics of Li-Po batteries well in monitoring changes in the battery system. In general, the model that is often used is the Thevenin battery model. In this study, the parameters in the Thevenin model, such as $R_o$ and $V_c$, are estimated using the RLS algorithm, while the OCV is estimated according to the terminal voltage value during the rest condition in the pulse test. The entire estimation process is carried out using a low-computing device, the Raspberry Pi Zero, with the help of an INA 260 sensor to read the battery current and voltage. The battery capacity used in this study is 5200mAh with a voltage of 11.1V. The pulse test device in this study uses a constant current discharge and a microcontroller device for the timing process. Before the voltage and current data are used for parameter estimation, the data is filtered using a one-dimensional Kalman filter. The estimation results for OCV, $R_o$, and $V_c$ show quite good performance, with an MSE value of $5.42 \times 10^{-6}$ V and an RMSE of 0.0023 V.



**Corresponding Author:**

Paris Ali Topan, Universitas Teknologi Sumbawa, Indonesia
Email: paris.ali.topan@uts.ac.id

## 1. INTRODUCTION

One type of battery that is widely used today for various applications with high energy density values and is lighter in weight is lithium polymer (Li-Po) [1]–[2]. This characteristic makes Li-Po batteries used in multiple modern electronic applications requiring high-capacity energy sources with compact sizes, such as mobile phones, laptops, and drones. In more advanced applications such as electric vehicles, Li-Po batteries can provide longer distances with efficient energy [3]–[4]. In the Energy Storage system (ESS) application for new renewable energy applications, this battery stores intermittent energy, whether household-based or in industrial facilities [5]–[6]. Li-Po battery performance is affected by the chemical conditions that will permanently change during use [7]–[8]. Hence, users need to know the chemical conditions of the Li-Po battery to determine energy efficiency and battery life. If this condition is not well known, it will result in a rapid degradation process in the battery cells and will reduce the battery's ability to store energy. In addition, the decline in the quality of chemicals in the battery will result in excessive heat on the surface. It can cause system failure and other hazards such as fire. In drone applications and devices used for medical purposes, unknown degradation values will cause sudden power loss, which is very detrimental, especially in conditions that require high reliability. Therefore, battery system users need to understand the chemical characteristics of the battery. Chemical degradation in batteries will be very difficult to observe [9], so a model is needed to represent

the chemical characteristics of the battery whose characteristics can represent the actual characteristics of the battery [10]. Several researchers have used several models to understand battery characteristics, and one of the most frequently used models is the Thevenin battery model [11], [12]. Thevenin battery model is one of several existing battery models, and it combines electronic components such as voltage sources, resistors, and capacitors to represent the chemical characteristics of Li-Po batteries [13]–[14]. The shape of the Thevenin model can be seen in Fig. 1.

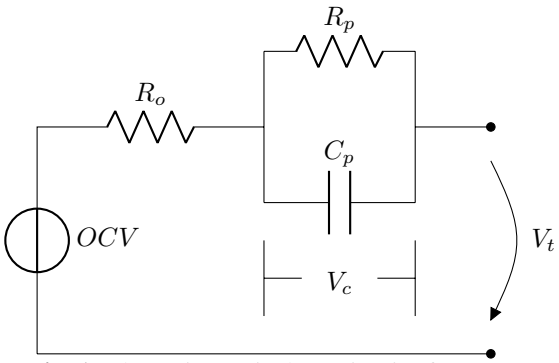


**Fig. 1.** Thevenin Equivalent Circuit of a Battery

Fig. 1 shows the structure of the Thevenin battery model, which consists of an $OCV$ voltage source that describes the battery voltage when the battery is not connected to the load [15], [16]. The $OCV$ voltage has an insignificant change compared to the voltage measured at the battery terminals, which changes significantly. The characteristics of this $OCV$ describe the mechanism of integration or disintegration of lithium ions in the battery that moves from or to the electrode material [17]–[18]. The next component is a resistor called internal resistance, labeled with $R_o$. This resistor describes the construction of chemicals in the battery, such as electrolyte material as a medium for lithium ions to move, the Solid Electrolyte Interphase Layer, and resistance to the electrode material [19], [20]. This internal resistance also causes a decrease in the measured voltage at the battery terminals, which is a significant decrease proportional to the current flowing. $R_p$ and $C_p$, arranged in parallel, describe the transient characteristics of the battery after a voltage drop occurs due to internal resistance and when the battery goes to the $OCV$ voltage after the current in the battery changes to current = $0A$ (disconnected from the load). Related to the chemical process in the battery, $R_p$ describes a resistance that occurs while moving lithium ions on the electrode surface. As for $C_p$, it describes the process of forming a double layer of electrons on the electrode, which then has a capacitance value [14], [21]. The simple structure of the Thevenin model makes it easy to use in simulations and efficient enough to be applied to devices that have limitations on the computing side, such as the Raspberry Pi Zero W. When compared to other models, such as the electrochemical model, which requires a complex calculation process so that it requires a device with high computing power, it is less suitable for actual application needs when compared to the Thevenin model. In addition, there is also a model based on neural networks or machine learning that models battery characteristics by performing a dataset training process, which will also require high computing.

The chemical characteristics represented by the electronic components of the Thevenin model can be determined by applying estimation algorithms such as Recursive Least Square (RLS) [22]–[23], Extended Kalman Filter (EKF) [12], [24], Artificial Neural Networks (ANN) [25], and several other estimation methods. RLS is the suitable algorithm for implementation in real applications with low computation because it is simpler and only requires a few computational resources so that it can be applied to embedded devices such as Arduino, ESP32, and Raspberry Pi Zero. For in-depth analysis purposes related to battery non-linearity, EKF is a good alternative because the probabilistic approach in the algorithm can handle nonlinear systems. However, it requires higher computing power compared to RLS. ANN can be used in the estimation process if there is extensive training data and high computing devices for initial training. The ANN algorithm is very effective in modeling very complex nonlinear relationships in batteries [26]. In the estimation process, RLS will analyze the voltage difference between the voltage measured at the positive and negative terminals of the battery and the voltage resulting from the estimation using the Thevenin model. Based on these differences, the RLS algorithm will update the parameter values of the Thevenin model to minimize estimation errors. The main advantage of RLS lies in its efficiency in updating parameters because it only uses the latest data in its algorithm without storing or processing the entire historical dataset. However, in the application of the RLS algorithm, several

challenges will be faced, such as estimation results that are affected by interference or noise in the input and output data used as a reference, which affects the accuracy of the estimation. Although RLS is very effective for linear or nearly linear systems, this algorithm could be more optimal in handling nonlinear systems.

Previous studies have tried using the Thevenin model to model Li-Po batteries, which were then estimated using RLS and several variants. Previous research [27] tried to identify lithium battery parameters based on changes in State of Charge (SoC) using the first-order Thévenin model. In that study, parameter identification was carried out starting from the battery SoC condition of 100% to 10%. Other research on Thevenin parameter estimation [28] tried to estimate by first collecting current and voltage data. An estimation process was carried out using the Least Square algorithm. The results obtained showed an absolute error value of 0.0052V. The study [29] tried to estimate SoC and State of Health (SoH) from the parameter estimation results in the Thevenin model using RLS. To obtain the SoC and SoH values, the Dual Extended Kalman Filter (DEKF) algorithm is used based on the estimated data using RLS. The testing method applied is Hybrid Pulse Power Characterization (HPPC) at different temperature conditions. Another study [30] tried to estimate SoC using an Adaptive Extended Kalman Filter (AEKF). Thevenin model parameters in the study were estimated using RLS and then entered into the AEKF equation applied to the LabVIEW application. Another RLS variant, namely variable forgetting factor recursive least squares (VFF-RLS), is used in several studies [31], [32], [33] to estimate Thevenin model parameters. In that research, the forgetting factor variable in the RLS algorithm is adjusted to the needs of each parameter to be estimated. In addition to using the standard Thevenin model, several studies also use different variations of the Thevenin model, such as in several previous studies [34]–[35], with the hope of being able to model better battery characteristics.

The estimation of Thevenin model parameters using the RLS method in previous studies used computer devices with very high computing capabilities; even some studies used software that required certain computer specifications. Such as Matlab [36], [37]. Using devices with advanced computing capabilities will take much work to apply to real applications such as Battery Management System (BMS) applications (Accurate Thevenin's circuit-based battery model parameter identification).

Using low-power computing devices to estimate parameter values in the Thevenin model using the RLS algorithm is very important in the actual estimation process, especially in modern applications today. Low-power devices aim to save energy on devices used in estimation, not to drain battery power significantly. Low device production costs are also necessary if the estimation device is commercialized. In addition, the small and portable size of the device will make it more accessible during the integration process with other supporting devices. The need for communication between devices using various communication protocols such as I2C, SPI, and other communication protocols is also critical, such as when the device communicates with current, voltage, and temperature sensor devices.

This study aims to estimate the parameters of the Thevenin model on Li-Po batteries using RLS applied to devices with low computing capabilities, namely Raspberry Pi Zero W. This approach is used as an alternative to high computing devices that have been used to estimate the parameters of the Thevenin battery model in real-time, using low computing devices. This study will provide new knowledge that Raspberry Pi Zero W can be an economical solution for real-time applications such as Battery Management Systems. This study also contributes to the real-time parameter estimation process: First, the Development of the RLS algorithm for battery parameter estimation for low-power devices so that it can be an alternative for cost savings. Second, this study will open up opportunities for direct application for real applications.

## 2. METHOD

### 2.1. Experimental Set-Up

The battery used in this study has a voltage specification of $11.1V$, the number of battery cells is 3S, C rate $25C$ to $50C$, with a capacity of $5200mAh$, and internal resistance in new conditions of 1 milliOhm - 5 milliOhm. The first step in the study is to charge the battery to total capacity or SOC = 100%, after which a test is carried out using the pulse test method. Pulse test testing is carried out by drawing current from the battery for ten seconds with a current of $0.5A$ with the help of a constant current discharger (CCD), then resting (where the current flowing from the battery to the discharger is $0A$) for 10 seconds as well. The timing in drawing current for a specific time and then resting is done automatically with the help of an XIAO ESP32 microcontroller, with the configuration shown in Fig. 2.

For safety in the data collection process, several things need to be considered regarding the use of Li-Po batteries, namely the polarity of the positive and negative voltages that must not be exchanged; if this happens, it will damage the device connected to the battery. In addition, with a large capacity and a significant C rate,

sparks can occur and experience extreme hot temperature conditions on the battery. As a result, the battery will be damaged. In this study, the battery and other devices are connected with an XT60 connector designed explicitly for battery connectors to minimize unwanted incidents.

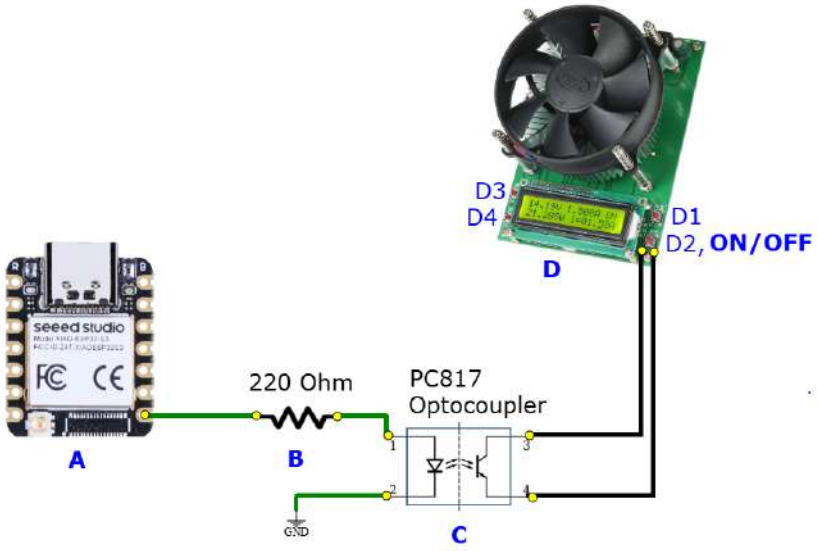


**Fig. 2.** Component A is the XIAO ESP32, which is responsible for controlling the discharger with the help of the PC817 optocoupler (Component C), whose output side is directly connected to the ON/OFF button (D2)

By default, the CCD used does not have the function to perform the pulse test process, so a simple modification is needed as shown in Fig. 2. In the picture, the microcontroller will be set to output a voltage on pin D7 of $5V$ for 10 seconds, then $0V$ for 10 seconds. Pin D7 is then connected to the PC817 optocoupler with a resistor as a current adjuster that enters pin 1 of the optocoupler of $220\,\Omega$. When the optocoupler is active (optocoupler input voltage $5V$), the Optocoupler output acts as a closed switch. When the input voltage is $0V$, it becomes an open switch. This phenomenon is then used to automatically control the CCD's physical ON/OFF button (in Fig. 2, the button is labeled D2).

Voltage and current measurements in this study used the INA260 sensor. This sensor can measure current on the low and high sides, with a maximum voltage of $+36V$ DC and a maximum current that can be measured at $15A$. This sensor was previously calibrated at the factory, so the current and voltage readings using this sensor are excellent in this research application. However, noise in the data can affect the estimation results. This sensor is connected to the Raspberry using the $I^2C$ protocol with a default address $0 \times 40$. Fig. 3 provides an overview of the connection between devices in this study. In Fig. 3, the battery whose model parameters will be estimated is connected to the CCD device via the INA260 sensor (positive cable only).

The current and voltage from the INA260 sensor are then read using the Raspberry Pi as the primary device in data processing. To read data from the INA260 sensor using the Raspberry Pi Zero, a Python script is written and executed on the Raspberry Pi using the Thonny IDE, which comes pre-installed with the Raspberry Pi Zero operating system. The Raspberry Pi specifications used in this study have a CPU processing speed of 1 GHz and 512 MB RAM, with dimensions of length: $65mm$ and width: $30mm$ [38]. This device supports several communication protocols that can be used in further developments [39], [40].

### 2.2. Preprocessing of Data

To handle noisy current and voltage data, the data first enters the one-dimensional Kalman filter algorithm before entering the RLS algorithm. This Kalman Filter algorithm is formed in a Python library, which is called in the main RLS program.

### 2.3. Thevenin model Equation

Thevenin battery model is formulated using equation (1). In equation (1), the model's output is the voltage $V_t$ measured at the positive and negative terminals of the battery, whose value corresponds to the amount of current flowing and is influenced by the voltage at $R_o$, $V_c$, and $OCV$.

$$V_t(k) - OCV(k) = -(I(k) \times R_o) - V_c \tag{1}$$

Where $V_t(k)$ is the voltage measured at time $k$ (the measurement result at that time) at the battery terminal read using the INA260 sensor, $OCV$k is the battery rest voltage at time $k$, and Ik is the battery current read using the INA260, $R_o$ is the internal resistance of the battery, and $V_c$ is the polarization voltage in the parallel circuit $R_p$ and $C_p$ to be estimated. In this study, only the $V_c$ value is estimated to see the influence of $R_p$ and $C_p$ arranged parallel in the Thevenin model. So, the dynamic properties of the Thevenin model due to the influence of $R_p$ and $C_p$ are not included in the formulation; this makes the Thevenin equation entered into the RLS algorithm not go through the discretization process using the Bilinear method or other discretization methods.

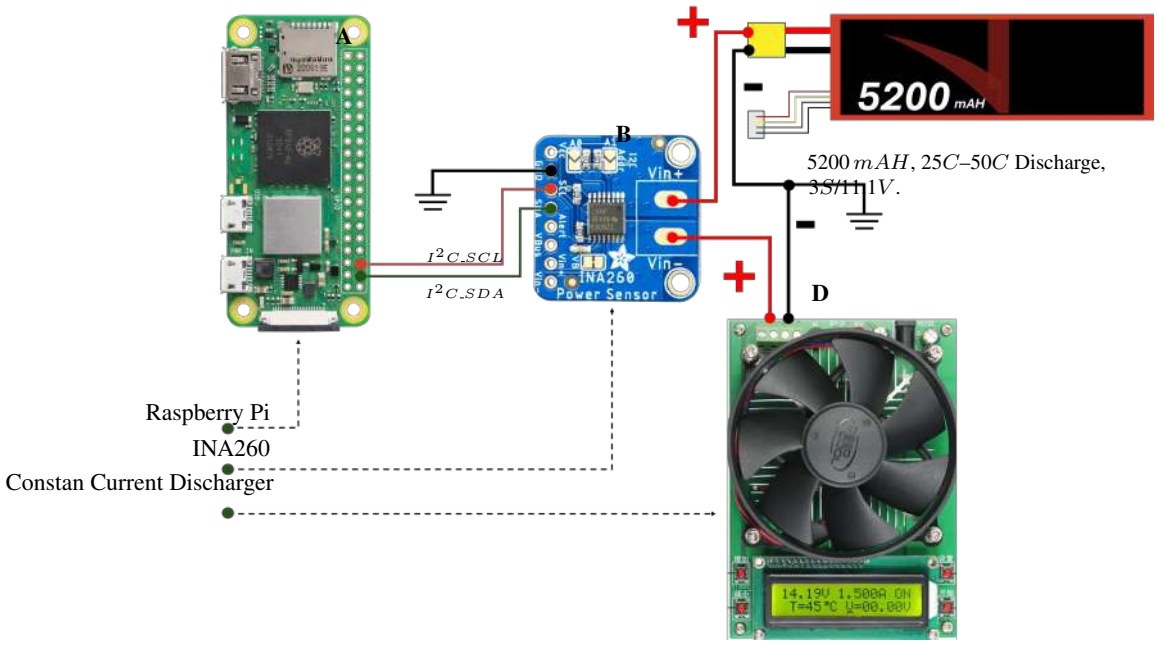


**Fig. 3.** Battery Data Testing Scheme

### 2.3.1. Determining the OCV Value

It should be noted that the $OCV$ value is the battery voltage value at a current condition of $0A$, or in the pulse test, the $OCV$ voltage is the voltage read at rest conditions. In this study, the $OCV$ value will be recorded at rest conditions only, while at current conditions greater than $0A$, the $OCV$ value will be the same as the $OCV$ value at the previous rest condition. Algorithm 1 is a Python pseudocode for the algorithm to determine the battery $OCV$ value. In Algorithm 1, the voltage and current used previously have been filtered using a one-dimensional Kalman filter, which is then stored in an $OCV$ variable and used for the following process. Fig. 4 shows the shape of the voltage and current during pulse test conditions, where the $OCV$ value is determined when the current condition = $0A$.

## 2.4. Recursive Least Square RLS

Equation (1) is then formed into an equation that can be entered into the RLS algorithm. Because the $OCV$ value is determined during the rest process in the pulse test and the terminal voltage and battery current values are obtained from the sensor, three variables in Equation (1) are known. Because the RLS equation requires an equation arranged in a matrix format, equation (1) is formed into a form of the equation given in Equation (3).

$$y(k) = V_t(k) - OCV(k) \tag{2}$$

$$y(k) = \begin{bmatrix} I(k) & 1 \end{bmatrix} \begin{bmatrix} -R_o \\ -V_c \end{bmatrix} \tag{3}$$

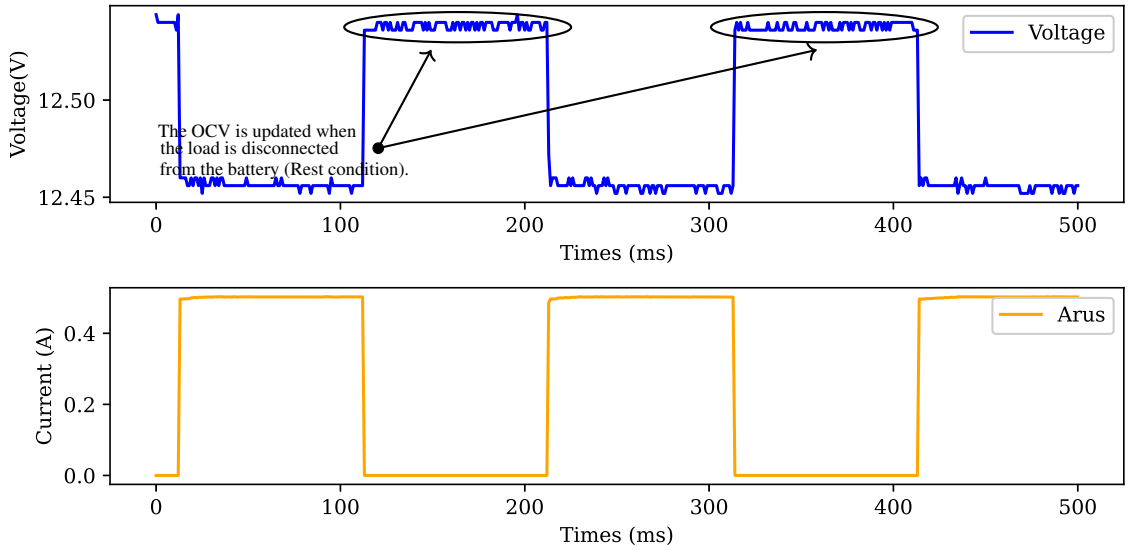


**Fig. 4.** Voltage and Current During Pulse Test Conditions

**Algorithm 1** OCV Estimation During Pulse Test

```
Initialize I²C for INA260 sensor
Define read_voltage() and read_current() functions to read data via I²C
Initialize variables:
    OCV = 0
    REST_THRESHOLD = 0.01
while True do
    V_t ← read_voltage()          ▷ Read terminal voltage from INA260
    I ← read_current()            ▷ Read current from INA260
    if |I| < REST_THRESHOLD then
        Set OCV = V_t             ▷ Assign the terminal voltage as OCV
    end if
end while
```

In the RLS algorithm, the first thing to do is to identify the parameters that will be input and output. From the equation of 3 input parameters in the form of current values represented by the vector $X(k) = \begin{bmatrix} I(k) & 1 \end{bmatrix}$, the output value is represented by $y(k)$, and the parameters to be estimated are $\theta = \begin{bmatrix} -Ro & -Vc \end{bmatrix}^T$. The initial value for $\theta$ in this study is $\begin{bmatrix} -0.01 & -0.01 \end{bmatrix}^T$. Then, the Thevenin model equation can be written briefly in the form of Equation (4).

$$y(k) = X(k) \cdot \theta \tag{4}$$

Next is to get the Gain value, which will later become a determining factor related to how much influence the new data from the INA219 sensor has on the estimation results. The equation to determine the gain value is given in Equation (5). In this equation, there is a forgetting factor value, the value of which is in the range of 0 to 1 ($0 < \lambda \leq 1$). The Forgetting factor value is profound in RLS to regulate how much the old data influences the estimation process. In this study, the Lambda value ($\lambda$) is set close to 1, which is 0.9999, with the aim of producing a stable estimation value, considering that the $R_o$ and $V_c$ values have properties that do not change too much.

$$K(k) = \frac{P(k-1)X(k)}{\lambda + X(k)^T P(k-1)X(k)} \tag{5}$$

For the initial value of the covariance matrix Pk in Equation (5) is given as $P(0) = 1000\times$ Identity Matrix with $n = 2$ or in its matrix form is $\begin{bmatrix} 1000 & 0 \\ 0 & 1000 \end{bmatrix}$. This Covariance value will determine the confidence level

in the initial value of the estimated parameter; the greater the value, the higher the level of uncertainty will be, but the estimation process will be more stable, and vice versa for smaller values.

The following process in the RLS algorithm is to update the $\theta$ parameters as the estimation results and update the covariance matrix values. The equations are given in Equations 6 and 7, respectively. Then, the pseudocode for the RLS algorithm can be seen in Algorithm 2.

$$\theta(k) = \theta(k-1) + K(k)\left(y(k) - X(k)^T\theta(k-1)\right) \tag{6}$$

$$P(k) = \frac{1}{\lambda}\left(P(k-1) - K(k)X(k)^T P(k-1)\right) \tag{7}$$

**Algorithm 2** RLS Algorithm for Battery Estimation

Initialize I2C for INA260 sensor
Define `read_current()` and `read_voltage()` functions for I2C communication
Initialize RLS parameters:
    $\lambda_{\text{rls}} = 0.99$ ▷ Forgetting factor
    $P = I \times 1000$ ▷ Covariance matrix
    $\theta = [R_o^{\text{init}}, V_c^{\text{init}}]$ ▷ Initial guesses for $R_o$ and $V_c$
    $OCV =$ open_circuit_voltage
**while** True **do**
    $V_t =$ `read_voltage()` ▷ Terminal voltage from INA260
    $I =$ `read_current()` ▷ Current from INA260
    $y_k = V_t - OCV$ ▷ Error between terminal voltage and OCV
    $X_k = [I, 1]$ ▷ Input vector for RLS
    Compute Kalman Gain:
        $K_k = \frac{PX_k}{\lambda_{\text{rls}} + X_k^T P X_k}$
    Update parameter estimates:
        $\theta = \theta + K_k(y_k - X_k^T\theta)$
    Update covariance matrix:
        $P = \frac{1}{\lambda_{\text{rls}}}(P - K_k X_k^T P)$
    $R_o^{\text{est}} = -\theta[0]$ ▷ Estimated $R_o$
    $V_c^{\text{est}} = -\theta[1]$ ▷ Estimated $V_c$
**end while**

The success of the RLS estimation results on the parameters in the Thevenin model will be measured using the Mean Squared Error (MSE) and Root Mean Squared Error (RMSE). MSE will calculate the average error between the actual measurement value, namely the battery terminal voltage measured by INA260, and the estimated terminal voltage value. At the same time, RMSE will show the difference between the terminal voltage measurement value and the predicted results in voltage units. Low MSE and RSME values indicate that the Thevenin model used can be considered close to the original characteristics of the battery.

### 2.5. Constraints and Further Research

Technical constraints faced in the research will be closely related to the programming process carried out directly on the Raspberry Pi Zero. Given that this device has a deficient computing speed, it will significantly affect the speed when opening the Thony IDE application as a place where the Python code is created. In addition to the noise that arises from the results of sensor readings, noise is also sometimes influenced by the condition of the cable connection between devices, which makes it very difficult to detect. The influence of the uncontrolled research environment temperature is also an obstacle in the research because the temperature is one of the parameters that affect battery characteristics.

For future research, it is necessary to create Python code outside the Raspberry Pi system or use other methods to facilitate the programming process. Creating a printed circuit board (PCB) for data collection devices must also be considered to eliminate noise in connecting devices. For the accuracy of the estimation process.

## 3. RESULT AND DISCUSSION

After carrying out the activities described in the research methodology, the next step is to analyze the results obtained. The results obtained in this study are in the form of $OCV$ parameter estimation results by observing the voltage values read from the INA260 sensor at rest conditions in the pulse test and the estimated $R_o$ and $V_c$ values estimated using the Raspberry Pi Zero device by applying the RLS algorithm. The data used during the estimation process is first filtered using a one-dimensional Kalman Filter to avoid errors in the estimation process. Fig. 5 shows the results of the battery pulse test. The graph displays the shape of the current read by the sensor due to the pulse test, and the shape of the battery terminal voltage graph is affected by changes in current. In addition, the graph in the figure also provides a graph of the terminal voltage of the RLS estimation results, which are then enlarged in detail to provide a better picture in Fig. 6.

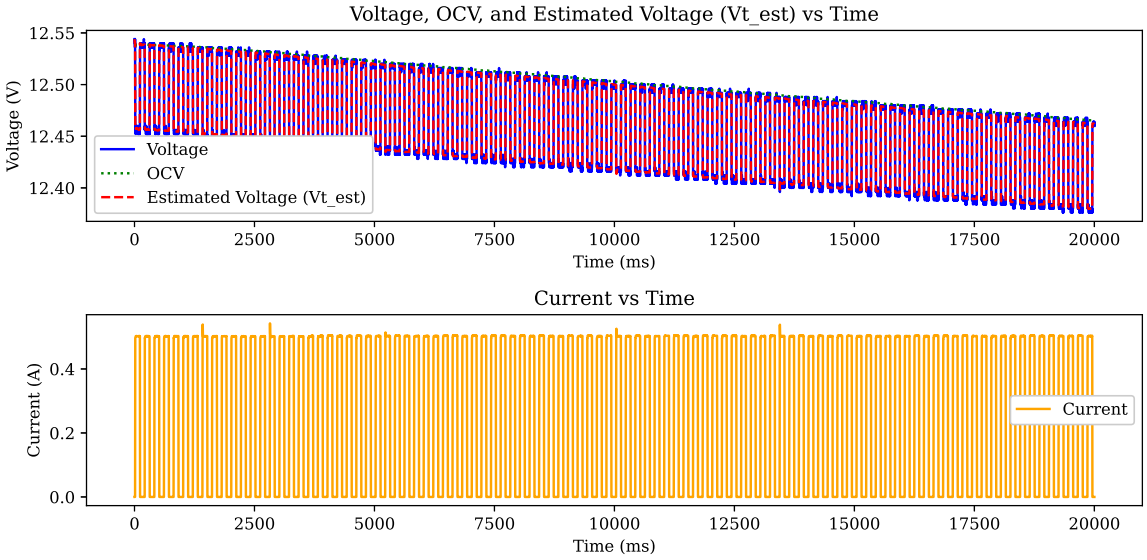


**Fig. 5.** Pulse test results on a $5200mAh$ battery, with a current of $0.5A$. The pulse test was conducted with a discharge duration of 10 seconds and a rest duration of 10 seconds

### 3.1. Results of OCV Value Estimation

The OCV value obtained from the voltage value at rest can be seen in the graph given in Fig. 6. The graph shows that the change in OCV value is insignificant (OCV in the graph is represented by a dashed green line). Note the graph when the battery current is 0.5A where the OCV voltage does not show a voltage drop effect that matches the nature of the OCV voltage on the battery.

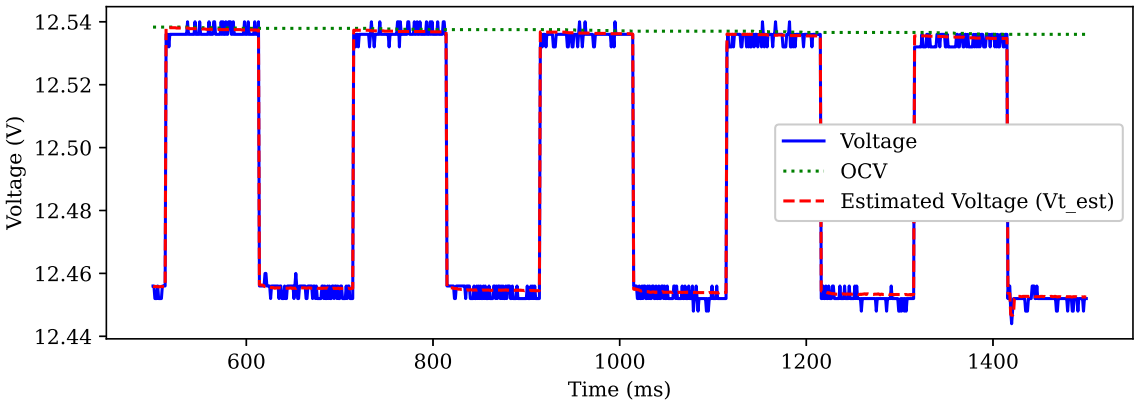


**Fig. 6.** The zoomed-in graph from Figure 4, which shows the estimated OCV and the estimated terminal voltage

The weakness of the OCV estimation when using this method lies in the timing of the pulse test. When the discharge time (current flowing from the battery is more than 0 A, or in this study 0.5 A) lasts longer, while the rest time is shorter, it will result in an error in estimating the OCV value. It should be noted that the longer the discharge time, the longer the time required for the voltage to reach the actual OCV value at rest conditions.

### 3.2. RLS Estimation Results for Ro and Vc.

The OCV value estimated in the previous stage is then entered into the RLS algorithm to estimate $R_o$ and $V_c$. The estimation results are then given in Fig. 7. The graph shown in Fig. 7 provides an overview of the $R_o$ and $V_c$ values. If seen from the results, the $R_o$ value is within the range of the internal resistance value of the battery (1 milli Ohm - 5 milli Ohm) in the new battery condition. The resulting $V_c$ value shows an exponential change that shows the dynamic nature of the battery.

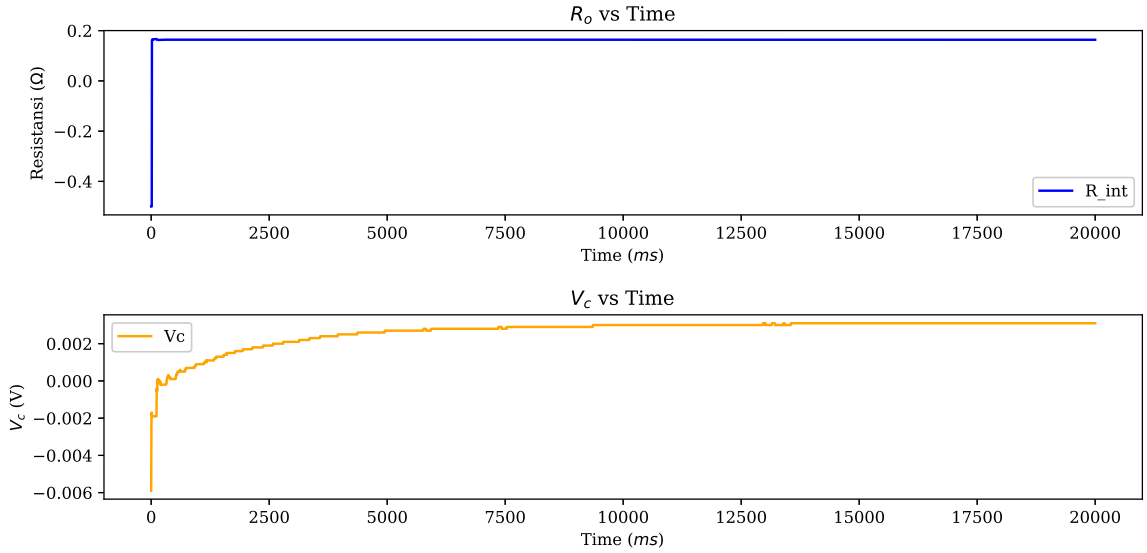


**Fig. 7.** RLS Estimation Results for Internal Resistance ($R_o$) and Polarization Voltage ($V_c$)

The problem experienced during the application of RLS is in selecting the forgetting factor value. In this study, the forgetting factor value will affect both estimated values, so if the forgetting factor value is not quite right, the stability of the estimation process on one of the estimated parameters will be affected. So, in further research, an RLS algorithm is needed to provide different and dynamic forgetting factor values for each parameter.

### 3.3. MSE and RMSE Results

The MSE value obtained in this estimation process is $5.42 \times 10^{-6}$, and the RMSE is $0.0023V$. The data used as the actual data is the terminal voltage value measured by the sensor after filtration using the one-dimensional Kalman Filter. So, if seen from the results of the MSE, it has a small value, likewise with the RMSE value, which is also quite small.

### 3.4. Results of Application on Raspberry Pi Zero

As the main objective of this study is to try to estimate the parameters of the Thevenin battery model on a device with low computing capabilities, namely the Raspberry Pi Zero, it has been successfully implemented starting from the process of reading INA260 sensor data, filtering data to the process of estimating$OCV$, $R_o$, $V_c$ parameters. However, there are still some things that need to be improved, especially in terms of direct application to the BMS system.

Furthermore, further research is needed to apply different algorithms in estimating parameters in the Thevenin model using the Raspberry Pi Zero, such as using other RLS variants or artificial intelligence methods. Determination of BMS parameters such as State of Charge (SoC), State of Health (SoH), and other BMS parameters, based on changes in the Thevenin model parameters, also needs to be studied when applied to low-computing devices such as the Raspberry Pi Zero.

## 4. CONCLUSION

This study has successfully implemented the RLS Algorithm on the Raspberry Pi Zero, which is used to estimate the parameters Ro and Vc, although some technical challenges are faced and need to be improved. The estimation of the value of the OCV parameter shows quite good estimation results both in resting conditions in the pulse test. The MSE value obtained is $5.42 \times 10^{-6}$, and the RMSE value of 0.0023 V indicates that the estimation error is quite small. In further research, it is necessary to conduct several further studies using other RLS variants or using artificial intelligence in estimating the value of the Thevenin model parameters, and the effect of environmental temperature on the estimation results of the Raspberry Pi zero device also needs to be studied, because the characteristics of the chemicals in the battery change according to temperature conditions.

## ACKNOWLEDGEMENT

The authors would like to express their sincere gratitude to the Directorate General of Higher Education, Research, and Technology, Ministry of Education, Culture, Research, and Technology of the Republic of Indonesia for the financial support in 2024 through the Beginner Lecturer Affirmation Research Program (Penelitian Dosen Pemula Afirmasi - PDP Afirmasi).

## REFERENCES

[1] J. M. A. Boadu and A. G. Elie, "Improved performance of li-ion polymer batteries through improved pulse charging algorithm," *Applied Sciences*, vol. 10, no. 3, p. 895, 2020, https://doi.org/10.3390/app10030895.

[2] Y. Miao, P. Hynan, A. von Jouanne, and A. Yokochi, "Current li-ion battery technologies in electric vehicles and opportunities for advancements," *Energies*, vol. 12, no. 6, p. 1074, 2019, https://doi.org/10.3390/en12061074.

[3] P. Makeen, H. A. Ghali, and S. Memon, "Investigating an influence of temperature and relative humidity on the electrical performance of lithium polymer ion battery using constant-current and constant voltage protocol at small scale for electric vehicles," in *11th International Conference on Power Electronics, Machines and Drives (PEMD 2022)*, vol. 2022, pp. 126–130, 2022, https://doi.org/10.1049/icp.2022.1030.

[4] V. Vaideeswaran, S. Bhuvanesh and M. Devasena, "Battery Management Systems for Electric Vehicles using Lithium Ion Batteries," *2019 Innovations in Power and Advanced Computing Technologies (i-PACT)*, pp. 1-9, 2019, https://doi.org/10.1109/i-PACT44901.2019.8959965.

[5] S. Sahoo and P. Timmann, "Energy Storage Technologies for Modern Power Systems: A Detailed Analysis of Functionalities, Potentials, and Impacts," in *IEEE Access*, vol. 11, pp. 49689-49729, 2023, https://doi.org/10.1109/ACCESS.2023.3274504.

[6] M. Javadi, X. Liang, Y. Gong and C. Y. Chung, "Battery Energy Storage Technology in Renewable Energy Integration: a Review," *2022 IEEE Canadian Conference on Electrical and Computer Engineering (CCECE)*, pp. 435-440, 2022, https://doi.org/10.1109/CCECE49351.2022.9918504.

[7] J. S. Edge *et al*., "Lithium ion battery degradation: what you need to know," pp. 8200–8221, no. 14, 2021, https://doi.org/10.1039/D1CP00359C.

[8] Z. Zhang, C. Ji, Y. Liu, Y. Wang, B. Wang, and D. Liu, "Effect of aging path on degradation characteristics of lithium-ion batteries in low-temperature environments," *Batteries*, vol. 10, no. 3, p. 107, 2024, https://doi.org/10.3390/batteries10030107.

[9] J. Guo, Y. Li, K. Pedersen, and D.-I. Stroe, "Lithium-ion battery operation, degradation, and aging mechanism in electric vehicles: An overview," *Energies*, vol. 14, no. 17, p. 5220, 2021, https://doi.org/10.3390/en14175220.

[10] S. E. O'Kane *et al*., "Lithium-ion battery degradation: how to model it," *Physical Chemistry Chemical Physics*, vol. 24, pp. 7909–7922, no. 13, 2022, https://doi.org/10.1039/D2CP00417H.

[11] C. -S. Huang and M. -Y. Chow, "Accurate Thevenin's circuit-based battery model parameter identification," *2016 IEEE 25th International Symposium on Industrial Electronics (ISIE)*, pp. 274-279, 2016, https://doi.org/10.1109/ISIE.2016.7744902.

[12] T. Hawsawi, M. Alolaiwy, Y. Taleb, A. Mezaael and M. Zohdy, "An Improved Thevenin Model-based State-of-Charge Estimation of a Commercial Lithium-Ion Battery Using Kalman Filter," *2023 IEEE Smart World Congress (SWC)*, pp. 735-741, 2023, https://doi.org/10.1109/SWC57546.2023.10448568.

[13] M. Lagraoui, M. Lhayani, A. Nejmi and A. Abbou, "A New Method for Identifying the Parameters of the Li-Ion Battery Thevenin Model," *2024 4th International Conference on Innovative Research in Applied Science, Engineering and Technology (IRASET)*, pp. 1-5, 2024, https://doi.org/10.1109/IRASET60544.2024.10549601.

[14] M. Hossain, S. Saha, M. E. Haque, M. T. Arif and A. Oo, "A Parameter Extraction Method for the Thevenin Equivalent Circuit Model of Li-ion Batteries," *2019 IEEE Industry Applications Society Annual Meeting*, pp. 1-7, 2019, https://doi.org/10.1109/IAS.2019.8912326.

[15] H. He, R. Xiong, and J. Fan, "Evaluation of lithium-ion battery equivalent circuit models for state of charge estimation by an experimental approach," *Energies*, vol. 4, no. 4, pp. 582–598, 2011, https://doi.org/10.3390/en4040582.

[16] S. Susanna, B. R. Dewangga, O. Wahyungoro and A. I. Cahyadi, "Comparison of Simple Battery Model and Thevenin

Battery Model for SOC Estimation Based on OCV Method," *2019 International Conference on Information and Communications Technology (ICOIACT)*, pp. 738-743, 2019, https://doi.org/10.1109/ICOIACT46704.2019.8938495.

[17] Y. Xu, X. Ge, R. Guo, C. Hu and W. Shen, "Electrode-Parameter-Based Fault Diagnosis and Capacity Estimation for Lithium-Ion Batteries in Electric Vehicles," in *IEEE Transactions on Industrial Electronics*, 2024, https://doi.org/10.1109/TIE.2024.3447749.

[18] D. Abbas, B. Boulebtateche and M. M. Lafifi, "Modeling of Lithium-ion battery open-circuit voltage using incremental and low current test," *2022 19th International Multi-Conference on Systems, Signals & Devices (SSD)*, pp. 2157-2162, 2022, https://doi.org/10.1109/SSD54932.2022.9955959.

[19] Y. Chen, X. Liu, G. Yang and H. Geng, "An internal resistance estimation method of lithium-ion batteries with constant current tests considering thermal effect," *IECON 2017 - 43rd Annual Conference of the IEEE Industrial Electronics Society*, pp. 7629-7634, 2017, https://doi.org/10.1109/IECON.2017.8217337.

[20] A. Benshatti, S. R. Islam, T. Link and S. -Y. Park, "Internal Resistance Measurement of Lithiumion Batteries using LC Resonant Tank," *2022 IEEE Applied Power Electronics Conference and Exposition (APEC)*, pp. 1085-1089, 2022, https://doi.org/10.1109/APEC43599.2022.9773510.

[21] A. Hentunen, T. Lehmuspelto and J. Suomela, "Time-Domain Parameter Extraction Method for Thévenin-Equivalent Circuit Battery Models," in *IEEE Transactions on Energy Conversion*, vol. 29, no. 3, pp. 558-566, 2014, https://doi.org/10.1109/TEC.2014.2318205.

[22] S. H. El-Sallabi, A. Sharida and S. S. Refaat, "Estimation of Lithium-ion Battery State of Charge Using Recursive Least Squares Method," *2024 4th International Conference on Smart Grid and Renewable Energy (SGRE)*, pp. 1-6, 2024, https://doi.org/10.1109/SGRE59715.2024.10428993.

[23] L. Li, W. Wang, X. Ding, Q. Chen and C. Zhang, "SOC Estimation of Li-ion Battery Based on VFFRLS-AEKF with Capacity Parameter," *2022 IEEE International Power Electronics and Application Conference and Exposition (PEAC)*, pp. 1069-1073, 2022, https://doi.org/10.1109/PEAC56338.2022.9959709.

[24] R. Hiremath, S. Hulakund, V. R. Torgal, A. Patil, H. R. Patil and A. B. Raju, "State-Of-Charge Estimation using Extended Kalman Filter," *2023 International Conference for Advancement in Technology (ICONAT)*, pp. 1-6, 2023, https://doi.org/10.1109/ICONAT57137.2023.10080761.

[25] Y. Mazzi, H. B. Sassi, F. Errahimi, and N. E. Sbai, "Pil implementation of adaptive gain sliding mode observer and ann for soc estimation," *Artificial Intelligence and Industrial Applications*, pp. 270–278, 2020, https://doi.org/10.1007/978-3-030-53970-2_25.

[26] T. Mayssae and B. I. Badr, "Performance Comparaison Of Lithium-Ion Battery Model Parameters Estimation Methods," *2024 4th International Conference on Innovative Research in Applied Science, Engineering and Technology (IRASET)*, pp. 1-7, 2024, https://doi.org/10.1109/IRASET60544.2024.10549192.

[27] M. Aminuddin, O. Wahyunggoro and A. I. Cahyadi, "Improving Battery Model Accuracy Through Parameter Identification Using RLS and Pulse Test Analysis," *2024 10th International Conference on Smart Computing and Communication (ICSCC)*, pp. 438-442, 2024, https://doi.org/10.1109/ICSCC62041.2024.10690426.

[28] M. Lagraoui, M. Lhayani, A. Nejmi and A. Abbou, "A New Method for Identifying the Parameters of the Li-Ion Battery Thevenin Model," *2024 4th International Conference on Innovative Research in Applied Science, Engineering and Technology (IRASET)*, pp. 1-5, 2024, https://doi.org/10.1109/IRASET60544.2024.10549601.

[29] Q. Li, H. Chen, S. Cai, L. Wang, H. Gu and M. Zheng, "State Estimation of Lithium-Ion Battery at Different Temperatures Based on DEKF and RLS," *2021 IEEE 16th Conference on Industrial Electronics and Applications (ICIEA)*, pp. 1619-1624, 2021, https://doi.org/10.1109/ICIEA51954.2021.9516414.

[30] M. Hossain, M. E. Haque, S. Saha, M. T. Arif and A. Oo, "State of Charge Estimation of Li-ion Batteries Based on Adaptive Extended Kalman Filter," *2020 IEEE Power & Energy Society General Meeting (PESGM)*, pp. 1-5, 2020, https://doi.org/10.1109/PESGM41954.2020.9282150.

[31] J. Ye, C. Wu, C. Ma, Z. Yuan, Y. Guo, R. Wang, Y. Wu, J. Sun, and L. Liu, "An adaptive peak power prediction method for power lithium-ion batteries considering temperature and aging effects," *Processes*, vol. 11, no. 8, p. 2449, 2023, https://doi.org/10.3390/pr11082449.

[32] M. A. A. Mohamed, T. Fai Yu and T. Grandjean, "PSO-Tuned Variable Forgetting Factor Recursive Least Square Estimation of 2RC Equivalent Circuit Model Parameters for Lithium-Ion Batteries," *2023 IEEE Vehicle Power and Propulsion Conference (VPPC)*, pp. 1-6, 2023, https://doi.org/10.1109/VPPC60535.2023.10403331.

[33] T. Zhu, S. Wang, Y. Fan, H. Zhou, Y. Zhou, and C. Fernandez, "Improved forgetting factor recursive least square and adaptive square root unscented kalman filtering methods for online model parameter identification and joint estimation of state of charge and state of energy of lithium-ion batteries," *Ionics*, vol. 29, pp. 5295–5314, 2023, https://doi.org/10.1007/s11581-023-05205-6.

[34] D. Deng, S. -Y. Liu, S. -L. Wang, L. -L. Xia and L. Chen, "An improved second-order electrical equivalent modeling method for the online high power Li-ion battery state of charge estimation," *2021 IEEE 12th Energy Conversion Congress & Exposition - Asia (ECCE-Asia)*, pp. 1725-1729, 2021, https://doi.org/10.1109/ECCE-Asia49820.2021.9479017.

[35] T. Białoń, R. Niestrój, and W. Korski, "Pso-based identification of the li-ion battery cell parameters," *Energies*, vol. 16, no. 10, p. 3995, 2023, https://doi.org/10.3390/en16103995.

[36] I. Jarraya, J. Loukil, F. Masmoudi, M. H. Chabchoub and H. Trabelsi, "Modeling and Parameters Estimation for Lithium-Ion Cells in Electric Drive Vehicle," *2018 15th International Multi-Conference on Systems, Signals & Devices (SSD)*, pp. 1128-1132, 2018, https://doi.org/10.1109/SSD.2018.8570620.

[37] T. Mayssae and B. I. Badr, "Performance Comparaison Of Lithium-Ion Battery Model Parameters Estimation Methods," *2024 4th International Conference on Innovative Research in Applied Science, Engineering and Technology (IRASET)*, pp. 1-7, 2024, https://doi.org/10.1109/IRASET60544.2024.10549192.

[38] S. M. Guertin, S. Vartanian and A. C. Daniel, "Raspberry Pi Zero and 3B+ SEE and TID Test Results," *2022 IEEE Radiation Effects Data Workshop (REDW) (in conjunction with 2022 NSREC)*, pp. 1-5, 2022, https://doi.org/10.1109/REDW56037.2022.9921679.

[39] Ö. S. Büyükçolak and R. Yeniçeri, "Quadrotor Model Implementation on Raspberry Pi Zero and Pi 4 Boards using FreeRTOS," *2023 12th Mediterranean Conference on Embedded Computing (MECO)*, pp. 1-4, 2023, https://doi.org/10.1109/MECO58584.2023.10154999.

[40] A. Huttunen *et al*., "Portable Low-Cost Fluorescence Reader for LFA Measurements," in *IEEE Sensors Journal*, vol. 20, no. 17, pp. 10275-10282, 2020, https://doi.org/10.1109/JSEN.2020.2992894.

## BIOGRAPHY OF AUTHORS

**Paris Ali Topan** The researcher's current focus is on Battery Management Systems (BMS). As a researcher in this field, he holds a Bachelor's degree in Electrical Engineering from the University of Mataram and a Master's degree in Electrical Engineering from Gadjah Mada University. Currently, he serves as a lecturer at the University of Technology Sumbawa, specifically in the Electrical Engineering Study Program. Email: paris.ali.topan@uts.ac.id.

**Dinda Fardila** The researcher is currently a lecturer in the Civil Engineering Program at Universitas Teknologi Sumbawa. The researcher completed their undergraduate degree (S1) at Universitas Muhammadiyah Yogyakarta, focusing on construction management. Continuing in the same field, the researcher pursued a master's degree (S2) at Universitas Gadjah Mada. Email: dinda.fardila@utsac.id.